



HAL
open science

Thermal Properties of New Insulating *Juncus Maritimus* Fibrous Mortar Composites/Experimental Results and Analytical Laws

Zahia Saghrouni, Dominique Baillis, Naïm Naouar, Nawfal Blal, Abdelmajid Jemni

► To cite this version:

Zahia Saghrouni, Dominique Baillis, Naïm Naouar, Nawfal Blal, Abdelmajid Jemni. Thermal Properties of New Insulating *Juncus Maritimus* Fibrous Mortar Composites/Experimental Results and Analytical Laws. Applied Sciences, 2019, 9 (5), pp.981. 10.3390/app9050981 . hal-02173002

HAL Id: hal-02173002

<https://hal.science/hal-02173002v1>

Submitted on 4 Jul 2019

HAL is a multi-disciplinary open access archive for the deposit and dissemination of scientific research documents, whether they are published or not. The documents may come from teaching and research institutions in France or abroad, or from public or private research centers.

L'archive ouverte pluridisciplinaire **HAL**, est destinée au dépôt et à la diffusion de documents scientifiques de niveau recherche, publiés ou non, émanant des établissements d'enseignement et de recherche français ou étrangers, des laboratoires publics ou privés.

Article

Thermal Properties of New Insulating Juncus Maritimus Fibrous Mortar Composites/Experimental Results and Analytical Laws

Zahia Saghrouni ^{1,*}, Dominique Baillis ², Naim Naouar ², Nawfal Blal ² and Abdelmajid Jemni ¹

¹ University of Monastir, National Engineering School of Monastir, Laboratory of Thermal and Energetic Systems Studies (LESTE), LR99ES31, Street Ibn ElJazzar 5019, Monastir, Tunisia; abdelmajidjemni1@gmail.com

² University Lyon, INSA-Lyon, CNRS UMR5259, LaMCoS, F-69621 Villeurbanne, France; dominique.baillis@insa-lyon.fr (D.B.); naim.naouar@insa-lyon.fr (N.N.); nawfal.blal@insa-lyon.fr (N.B.)

* Correspondence: zahiasagrouni@yahoo.fr; Tel.: +216-23-528-960

Received: 25 January 2019; Accepted: 19 February 2019; Published: 8 March 2019



Abstract: This study aims to study the thermal properties and the microstructure of composite materials based on mortar combined with *Juncus maritimus* fibers. Effective thermophysical properties of the composite materials containing *Juncus maritimus* fibers are experimentally and theoretically investigated. To better understand the morphology of these new composites, the corresponding microstructures were characterized in 2D by scanning electron microscope and in 3D using micro computed tomography. The local thermal conductivity of the *Juncus maritimus* fibers was identified using theoretical models and experimental measurement of the effective thermal conductivity of packed bed of crushed fibers. The thermal conductivity of the mortar matrix at given porosity was also determined using experimental measurement data and a theoretical model. The most appropriate analytical laws to predict effective thermal conductivity of mortar composites containing fibers are deduced from experimental thermal conductivity results.

Keywords: thermal insulation; composite material; mortar; *Juncus maritimus*; thermophysical properties; thermal conductivity; micro computed tomography; thermal analytical modeling

1. Introduction

The development of building construction materials using agricultural residues and natural media presents a great interest. Indeed, such materials are useful to limit the energy consumption of the building and to reduce the environmental impact. They present other advantages such as renewability, biodegradability, low density and availability with low cost. Research activities on these materials are increasing these last years. Among them, some works in literature are focused on the thermal characterization of green insulating porous material [1,2] such as cellulose based aerogel [3,4], and composite materials using natural fibers such as Hemp shives [5–8], Flax and straw rape [8], granular cork [9,10] and palm date fibers [1,2,11,12]. Currently, composite materials have various applications in buildings; in walls, floors and roofs for insulation. Some studies showed that the natural materials embedded in different construction materials (such as plaster, cement, and mortar) allow good thermal insulating performances [13].

The influence of natural fibers content and size on effective thermal conductivity of composite materials has been analyzed [1,14,15]. For example, Ben Mansour et al. [1] conducted an experimental investigation of the thermal and mechanical properties of composites of mortar mixed with date palm fibers (DPF) by varying the content and the size of the added fibers. They showed that the DPF size does not have significant influence, while having a higher DPF fiber content improves thermal insulation

capacity. For DPF loading lower than 15 wt%, the mortar composite represents a good compromise between both thermal and mechanical performance of construction materials. These previous works underlined the importance to study the effect of fiber content on thermal conductivity of composites.

Other works present comparison between effective thermal conductivity experimental and analytical model results [5,9]. The data of analytical models are the fiber volume fraction or porosity and the thermal conductivity of each phase constitutive of composite materials [16,17]. They are useful to analyze the influence of fiber density, but on the other hand, they required the knowledge of local thermal conductivity. Thus, recently some works in literature are interested in the measurement of thermal conductivity of hemp fiber packed bed [18,19]. Other works investigated the thermal conductivity of the solid phase of the hemp shives [8,19].

In this context, this current study investigates new insulating mortar composites containing *Juncus maritimus* fibers. *Juncus maritimus* (Var. *typicus*) is a natural plant growing easily in wet and aquatic places, it counts 200 species of *Juncus* plant belongs to the family of Juncaceae according to Lisse et al. [20]. It is worth mentioning that there was no previous work concerning the *Juncus maritimus* fibers used as reinforcement in a mortar in order to improve its thermal insulating efficiency. We aim to take advantage of these renewable resources to develop new lightweight composites having the same concept and application as the Hemp concrete [2,13]. The fibers derived from the *Juncus maritimus* plant are expected to be a good substitute of Hemp fibers considering the availability of this plant throughout the year, while, harvesting the Hemp fibers is periodic. Moreover, there is a low gray energy in the manufacturing of the composite mortar containing *Juncus maritimus* fibers.

In this current work, different samples containing weight fractions of fibers ranging from 0% to 10% are studied. The microstructure of samples is characterized in 2D by SEM and in 3D by micro computed tomography (μ CT). We work on both experimental thermal characterization and theoretical analytical models. Effective conductivity and diffusivity of the sample are measured. An approach is proposed to estimate thermal conductivities of mortar matrix and also the local thermal conductivity of crushed *Juncus maritimus* (JM) fibers (JM local thermal conductivity). Then, based on these data and on the sample microstructure analysis, analytical models currently used in the literature [21–23] are tested and compared with effective thermal conductivity measurements. Appropriate analytical models are deduced to predict thermal conductivity of new composites.

2. Materials and Experimental Characterizations

2.1. Description of Basic Materials

Rush stem (*Juncus maritimus*) is a perennial plant shown in Figure 1. The used rush stems have an average length about 1 m with average diameter 2.5 mm. Some chemical composition of rush stems derived from Tunisian regions are reported in Table 1.



Figure 1. Rush stems (*Juncus maritimus*).

Table 1. Chemical composition and physical of rush stems derived from Tunisian regions [24].

Rush	Chemical Composition					Physical Properties
	Ash (%)	Hemicellulose (%)	Cellulose (%)	Holocellulose (%)	Lignin (%)	Humidity (%)
JcMoNc	7.3	27.84	40.99	68.84	18.54	10.22
JcAmHs	5.29	35.36	53.10	88.46	13.05	8.55

The sand used in manufacturing the composite samples is sieved at a maximum size of 1 mm. The used cement is Portland cement CEMII/A-L32.5R according to the Tunisian standard NT 47-01:1983 [25] and the European EN 197-1: 2000 [26], used in wall's manufacturing. The chemical composition of the used cement is presented in Table 2.

Table 2. Chemical composition of Portland cement CEMII/ A-L 32.5 R.

Material	CaO (%)	SiO ₂ (%)	Al ₂ O ₃ (%)	Fe ₂ O ₃ (%)	MgO (%)	SO ₃ (%)	Loss on Ignition (%)
cement	66.3	21.1	4.9	2.7	1.0	2.6	5.5

As for the mortar boards, they are made by mixing 2/3 of sand and 1/3 of cement with water to cement ratio (W/C) of 0.7.

2.2. Composite Preparation

In order to improve the thermal properties of mortar, the *Juncus maritimus* fibers were used to replace an equivalent percentage in mass (2%, 5%, 7%, and 10%) of cement and sand in mixture used in manufacturing of classical mortars.

The stems of *Juncus maritimus* were dried under natural conditions for two days then in an oven regulated at 70 °C for 8 hours until a constant weight. After that, the stems of *Juncus maritimus* were ground in a mechanical crusher in order to improve the adhesion interface between fibers and mortar paste. The obtained product was then sieved using mesh size comprised between 1 mm and 2.5 mm (Figure 2).



Figure 2. Crushed fibers.

The composite samples were obtained by mixing cement, sand and *Juncus maritimus* fibers with different weight fractions of fibers (0%, 2%, 5%, 7%, and 10%) and water. The sand and cement were initially mixed at low speed. The *Juncus maritimus* fibers were gradually added to the dry mixture, while continuing the mixing. Then, the water was gradually added without stopping the mixing. The homogenized mixture was manually introduced into parallelepiped molds (27 cm × 27 cm × 3 cm). After two days, the samples were removed from the molds and dried in laboratory conditions for 28 days. Then, the samples were dried in an oven regulated at 60 °C for 3 days until constant weight.

2.3. Apparent Density Measurements

The density of mortar composites, ρ_c , was calculated by dividing the mass of the sample by its volume. Each sample's weight was measured by an electronic balance (Mettler-Toledo, LESTE Laboratory, Monastir, Tunisia) with (0.01 g precision) and its size is determined using a caliper square.

Then, a vessel of volume 400 mL was filled with crushed *Juncus maritimus* fibers. Measuring the mass of the amount of the crushed fibers and knowing volume of the container, the apparent density of the *Juncus maritimus*, $\rho_{a,JM}$, was determined. The value obtained is 295.6 kg/m³.

2.4. *Juncus Maritimus* Fibers Density and Porosity Determination

Crushed Fibers Samples' Porosity and *Juncus Maritimus* Fibers Density Measurements

The inter-particle porosity, ϕ_{inter} , is determined from the apparent density of crushed fibers samples, $\rho_{a,JM}$, and the *Juncus maritimus* fibers' density, $\rho_{s,JM}$, using pycnometer method (which consists of filling the space between fibers with Carbon tetrachloride CCl₄ except the discrete pores inside the fibers). The inter-particle porosity was expressed as follows:

$$\phi_{inter} = 1 - \frac{\rho_{a,JM}}{\rho_{s,JM}} \quad (1)$$

The values obtained for the density, $\rho_{s,JM}$, and the interparticle porosity, ϕ_{inter} , are 987.01 kg/m³ and 70.05%, respectively.

2.5. *Juncus Maritimus* and Solid Mortar Volume Fraction Determination

The *Juncus maritimus* volume fraction, $\varphi_{JM,v}$, contained in the composite materials is determined using the density values, ρ_C , $\rho_{s,JM}$, and the fiber mass fraction, $\varphi_{m,JM}$. It is expressed as follows:

$$\varphi_{JM,v} = \frac{\rho_C}{\rho_{s,JM}} \varphi_{m,JM} \quad (2)$$

The dense mortar volume fraction, $\varphi_{m,v}$, was also determined using the solid density, ρ_s , of mortar matrix, its mass fraction, $\varphi_{m,m}$, and composite density, ρ_c . It is expressed as follows:

$$\varphi_{m,v} = \frac{\rho_c}{\rho_s} \varphi_{m,m} \quad (3)$$

where the solid density of mortar, ρ_s , was determined from the dry density, ρ_0 and the measured porosity, ϕ_0 , of the reference mortar sample (without fibers) and it is expressed as follows:

$$\rho_0 = (1 - \phi_0) \rho_s \quad (4)$$

Indeed, the effective porosity of the reference mortar (without fibers), ϕ_0 , was measured directly using the Helium gas expansion porosimeter-UltraPoreTM300 [27]. The pore volume was determined using the isothermal Helium expansion and by application of the Boyle's law.

The value obtained for the porosity, ϕ_0 , and the solid density, ρ_s , of reference mortar are 27% and 2647.94 kg/m³, respectively.

Thus, the porosity of composite samples is deduced and is expressed as follows:

$$\phi = \frac{V_p}{V_t} = \frac{V_t - V_{JM} - V_m}{V_t} = 1 - \varphi_{JM,v} - \varphi_{m,v} \quad (5)$$

2.6. Microstructural and Morphological Analysis of Samples Containing *Juncus Maritimus* Fibers

2.6.1. SEM Analysis

Scanning Electron Microscope (SEM) was used to characterize the morphology of the crushed *Juncus maritimus* fibers (that will be used in the mixture) and the *Juncus maritimus*/mortar composites. The crushed fibers and the composites were fixed on silver plates. Then, they were coated with a fine layer of gold in a vacuum chamber to make it conductive.

Scanning microscopy analysis of crushed *Juncus maritimus* fibers with cylindrical shape is shown in Figure 3.

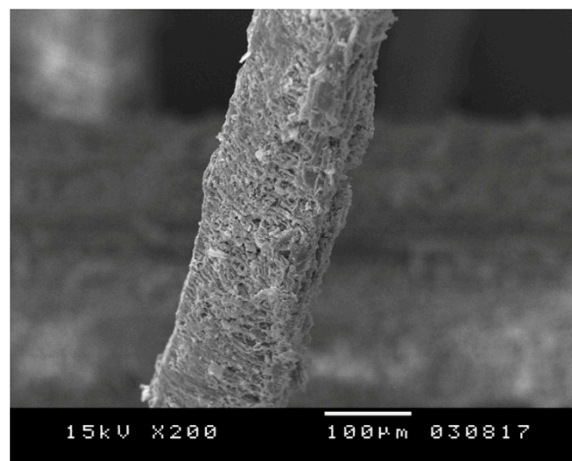


Figure 3. SEM image of crushed *Juncus maritimus* fibers.

Figure 4a shows SEM micrographs of the reference mortar (without fibers). Sand particles are embedded in cement. It can be seen some voids in reference mortar. Thus reference mortar is a porous media. Figure 4b shows *Juncus maritimus* fibers dispersed in the mortar matrix. It can be also observed that the porosity increases.

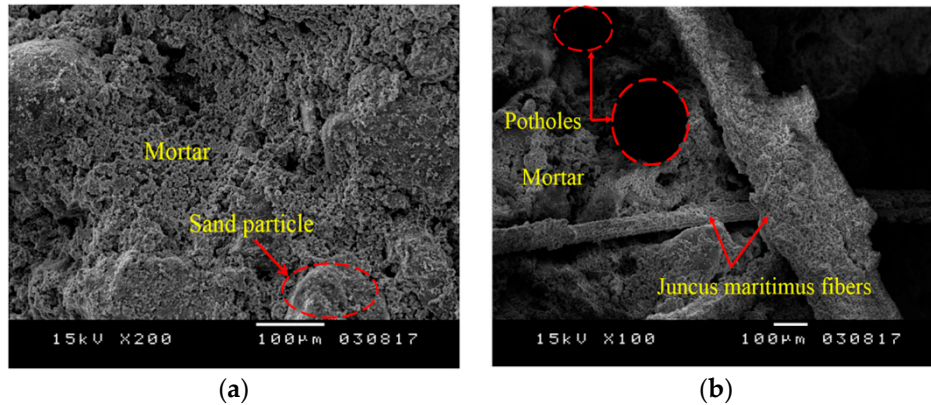


Figure 4. Scanning electron microscopy images: (a) Reference mortar (without fibers); (b) *Juncus maritimus*/mortar composites.

2.6.2. Micro Computed Tomography Analysis

The micro computed tomography imaging allows obtaining non-destructive 3D images of the materials. Images were acquired using a laboratory tomography Phoenix V tome X (Mateis, INSA Lyon, France). In our case, the resolution is adjustable from 1 to 5 μm . The detector used is made of 1920×1575 pixels each with a size of $127 \times 127 \mu\text{m}$. Imaging scans were performed using beam values close to 20 KeV and 170 μA without additional filter.

The 3D micro computed tomography (μCT) images reveal air pores entrapped inside the reference mortar (mortar without fibers) with globally spherical shape (Figure 5a,b). Figure 5c,d show detail view of sample composites filled with 5 wt% and 10 wt% fibers. We can see pores created by the incorporation of the fibers in the mortar mixture. The 3D- μCT images show also fibers randomly dispersed in the mortar mixture (Figure 5c,d).

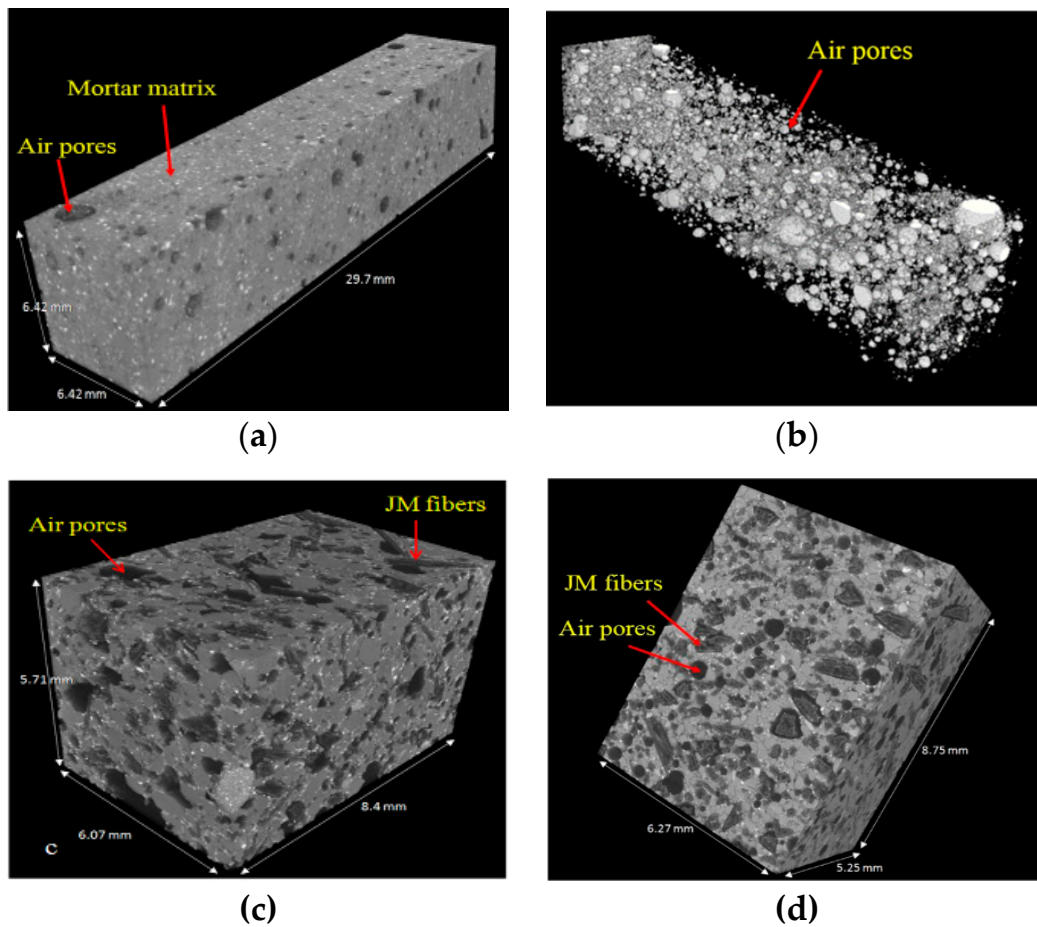


Figure 5. 3D-micro computed tomography (μ CT) images of composites: (a) Reference mortar (Resolution 1 voxel = 22 μ m); (b) pores in the reference mortar; (c) composite with 5 wt% of fibers ((Resolution 1 voxel = 7 μ m); (d) composite with 10 wt% of fibers (resolution 1 voxel = 7 μ m).

2.7. Thermal Characterization Method

The testing apparatus used in this work to evaluate the thermal conductivity and the thermal diffusivity of composites and crushed fibers is the boxes method. It is used in the recent publications [12,15,28] to determine the thermal properties of building composite materials. This device is constituted of two boxes, one is used to measure the thermal conductivity and the second is used to determine the thermal diffusivity in a transitory state.

2.7.1. Thermal Conductivity of Composite Samples

The thermal conductivity of bricks was determined in steady-state of the box method. The test sample was placed between an electrically heated box at temperature, T_h and a cold box that was maintained at a cold temperature, T_c , equipped with a cryostat-controlled heat exchanger. The lateral sample faces were insulated with extruded polystyrene in order to avoid heat loss and to impose a unidirectional heat transfer. The device was equipped with four temperature sensors connected to an acquisition card allowing to measure and record the hot temperature, the cold temperature, the ambient temperature of the room, T_a , and the temperature of the box, T_b . When the steady state was established, the temperature gradient between the two faces of the sample was measured. The effective thermal conductivity of the sample was calculated from the Fourier's relation (Equation (6)):

$$k = \frac{qe}{S\Delta T} = \frac{e}{S\Delta T} \left(\frac{U^2}{R} - C\Delta T' \right) \quad (6)$$

Where:

$$\Delta T = T_h - T_c \tag{7}$$

$$\Delta T' = T_b - T_a \tag{8}$$

2.7.2. Effective Thermal Conductivity of the Crushed Juncus Maritimus Fibers Measurement

The Juncus maritimus crushed fibers were placed in a sample holder which is composed of two copper plates and four sides, which are in Plexiglas. We introduced the crushed Juncus maritimus fibers into the enclosure through a series of vibrations and compressions in order to obtain perfect contact between copper plates and fibers. The choice of copper is justified by its high thermal conductivity which is equal to 389 W/m·°C. The Plexiglas has a low thermal conductivity k_p compared to copper, its value 0.2 W/m·°C. Hence, the heat flow was directly applied to the packed bed of the Juncus maritimus particles and heat transfer was considered unidirectional through the material of dimension $27 \times 27 \times 3 \text{ cm}^3$. The relationship of the thermal conductivity measurements (taking into account the box surfaces) proposed by [29], expressed as follows is used:

$$k = \frac{S_T}{S_{JM}} k_{mes} - \frac{S_p}{S_{JM}} k_p \tag{9}$$

where:

S_{JM} : Area occupied by Juncus maritimus fibers

S_p : Plexiglas area

$$S_T = S_p + S_{JM}$$

2.7.3. Thermal Diffusivity Measurement of Composites and Crushed Fibers

For thermal diffusivity measurements, the sample is placed in the second box which is equipped with a halogen lamp of 1000 W. The thermal diffusivity of the samples and the fibers were determined by the flash method. The measuring principle consists in applying a pulse with a short duration on the bottom face of the specimen and recording the temperature evolution on the opposite face (not irradiated face) as a function of time. The thermal diffusivity was identified from experimental thermogram and theoretical model in literature [30]. As an example the thermograms of crushed fibers packed bed (with inter particle porosity equal to 70.05%) and reference mortar (without fibers) samples are shown in Figure 6. It can be observed that the evolution of the temperature until to reach up the maximum value inside the packed bed of the crushed fibers is very slow compared to that of the reference mortar. These results tend to show that the crushed fibers are more resistant to heat propagation than the reference mortar.

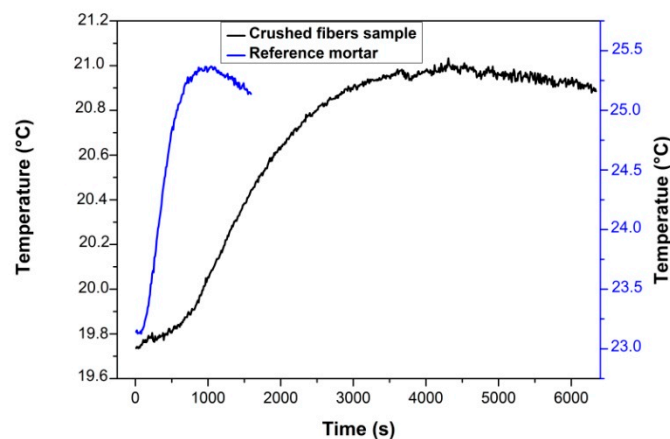


Figure 6. Experimental thermogram of opposite faces of crushed fibers and reference mortar sample.

3. Results and Discussions

3.1. Macroscopic Physical Properties of the Composites

Table 3 presents the measured value of dry density and the porosity values of different composite samples obtained from Equation (5). It is observed that the density of composite samples decreases with increasing fiber content in the mortar matrix. The introduction of these short fibers induces increasing voids of air into the materials. Regarding porosity determination results, values increase as the fibers content increases. For example, at 10 wt% of *Juncus maritimus* fibers, the value of porosity is about 52.22% is almost two times higher than the reference mortar. It is worth noting that the inclusion of fibers into the mortar matrix enhance the lightness of the building materials.

Table 3. Physical properties of composite samples; JMC0, JMC1, JMC2, JMC3, JMC4 are the *Juncus maritimus*/mortar samples corresponding to the *Juncus maritimus* mass fractions (0, 2%, 5%, 7%, and 10%), respectively.

Sample	JMC0	JMC1	JMC2	JMC3	JMC4
Mass ratio of <i>Juncus maritimus</i> to mortar mixture (%)	0	2	5	7	10
<i>Juncus maritimus</i> volume fraction (%)	0	3.1	6.6	8.8	11
Dry density (kg/m ³)	1933	1540.76	1302.6	1236.52	1081.96
Calculated porosity ϕ (%)	27	39	43	47.77	52.22

3.2. Thermal Properties of Crushed *Juncus Maritimus* Fibers and Mortar Composites

The measured value of thermal conductivity and thermal diffusivity of the packed bed of crushed *Juncus maritimus* fibers are $k_{JM,eff} = 0.09 \pm 0.0024$ W/m·K and $\alpha_{JM,eff} = (1.2 \pm 0.04) \times 10^{-7}$ m²/s, respectively, with inter particle porosity equal to 70.05%. It can be noted these values are close to properties of packed bed wood shaving with $k = 0.085$ W/m·K, $\alpha = 0.69 \times 10^{-7}$ m²/s [31].

3.3. Effect of Fibers Content on Composite Thermal Conductivity and Thermal Diffusivity

Table 4 presents the effective thermal conductivities, k_{eff} , and diffusivities, α , of the samples reinforced with different fiber loadings. We can see that the thermal conductivities decrease with increasing the fiber mass ratio. In fact, the values decreased from 0.521 W/m·K to 0.171 W/m·K when the percentage of *Juncus maritimus* fibers mass ratio increases from 0% to 10%. This reduction could be explained by the low thermal conductivity of the *Juncus maritimus* fiber compared to mortar matrix. Another explanation point out that the introduction of the *Juncus maritimus* particle in the mortar matrix leads to increase the porosity of composite samples. Similarly, the thermal diffusivity decreases simultaneously with the increase of fiber content by up to 37%.

Table 4. Thermal conductivity and thermal diffusivity of composite samples for different mass fraction.

Fibers loading (wt%)	k_{eff} (W/m·K)	α (m ² /s)
0	0.521 + 0.0036	$2.6 \times 10^{-7} \pm 0.015$
2	0.445 ± 0.005	$2.53 \times 10^{-7} \pm 0.006$
5	0.236 + 0.001	$2.01 \times 10^{-7} \pm 0.1$
7	0.197 + 0.0004	$1.73 \times 10^{-7} \pm 0.06$
10	0.171 + 0.00223	$1.623 \times 10^{-7} \pm 0.016$

Table 5 illustrates a comparison between the thermal properties and the densities of *Juncus maritimus*/ mortar composites which are investigated in this work and other materials used for the thermal insulation in buildings. It is clear that the thermal conductivity for *Juncus maritimus* (JM) /mortar composites (10 wt%) are lower than the mortar composites filled with other natural fibers such as wood shavings (30 wt%) [28], and date palm mesh (DPF) (51 vol.%) [12] while the thermal

diffusivity is almost constant for these three composites. The JM/mortar composites exhibit also a good thermal performance compared to mortar/cork composites [32]. It is interesting to highlight that the thermal conductivity of the JM/ mortar are close to the Hemp concrete which is available on the market ($0.17 \text{ W/m}\cdot\text{K} < k_{\text{eff}} < 0.48 \text{ W/m}\cdot\text{K}$) [33].

Table 5. Comparison of the thermal properties of Juncus maritimus/mortar composites and some building materials used for thermal insulation. DPF: date palm mesh.

Material	K_{eff} (W/m·K)	α ($\times 10^{-7} \text{ m}^2/\text{s}$)	ρ_c (Kg/m ³)	References
Reference mortar	0.521	2.6	1933	[This work]
JM/mortar (10%)	0.171	1.623	1081.96	[This work]
Wood/mortar (30%)	0.24	1.5	1495	[31]
DPF mesh/mortar (51%)	0.243	1.5	1217	[13]
Cork/mortar (10%)	0.96	-	2100	[32]

3.4. Analytical Modeling of the Effective Thermal Conductivity

To estimate the effective thermal conductivity of heterogeneous materials using analytical models, the knowledge of thermal conductivities of each phase constitutive of materials are required. However, the thermal conductivities of solid phases are unknown parameters as it is difficult to measure them directly. Thus, identification method based on the fitting between theoretical and experimental effective thermal conductivity results are required to determine the unknown phases properties.

3.4.1. Effective Thermal Conductivity of Porous Mortar

The 3D- μ CT images (Figure 5a,b) reveal that the reference mortar is constituted of two phases: the continuous solid phase: sand and cement mixture, and the dispersed phase: air spherical pores randomly distributed in mortar matrix. The Hadley model [34] that combines the Maxwell upper bound with an adjustable function $f_0(\phi)$, is applied to the medium made of the fluid phase “f” surrounded by a solid matrix “s”.

The thermal conductivity, k_s , of the solid phase of reference mortar (without fiber) is identified using the following Hadley expression (Equation (10)) and reference mortar effective thermal conductivity measured experimentally:

$$\frac{k_e}{k_f} = (1 - \alpha_0) \frac{\phi f_0 + \frac{k_s}{k_f} (1 - \phi f_0)}{1 - \phi(1 - f_0) + \phi(1 - f_0) \frac{k_s}{k_f}} + \alpha_0 \frac{2 \left(\frac{k_s}{k_f}\right)^2 (1 - \phi) + (1 + 2\phi) \frac{k_s}{k_f}}{(2 + \phi) \frac{k_s}{k_f} + 1 - \phi} \tag{10}$$

Where ϕ is the porosity of samples, k_f is the air thermal conductivity and the coefficients f_0 and α_0 are given by:

$$f_0 = 0.8 + 0.1\phi \tag{11}$$

$$\begin{cases} \log \alpha_0 = -4.898\phi & 0 \leq \phi \leq 0.0827 \\ \log \alpha_0 = -0.405 - 3.154(\phi - 0.0827) & 0.0827 \leq \phi \leq 0.298 \\ \log \alpha_0 = -1.084 - 6.778(\phi - 0.298) & 0.298 \leq \phi \leq 0.58 \end{cases} \tag{12}$$

Using the measured effective thermal conductivity of the reference mortar $k_e = k_{\text{eff}} = 0.521 \text{ W/m}\cdot\text{K}$ obtained $\phi = 0.27$ and $k_f = 0.026 \text{ W/m}\cdot\text{K}$, the inversion of Equation (10) leads to determine the solid thermal conductivity of dense mortar: $k_s = 2.868 \text{ W/m}\cdot\text{K}$.

Then, knowing k_s , this model is used to calculate the effective thermal conductivity of porous mortar, k_e , for different porosities. Results are presented in Table 6.

Table 6. Thermal conductivity of porous mortar for different porosity.

Fibers Loading (wt %)	Porosity (ϕ)	K_e (W/m·K)
0	0.27	2.868
2	0.39	0.399
5	0.43	0.239
7	0.47	0.211
10	0.52	0.182

3.4.2. Estimation of the Local Juncus Maritimus Thermal Conductivity from Crushed Fibers Effective Conductivity

This section focuses on the thermal conductivity determination of the local Juncus maritimus fibers. This property is identified by fitting theoretical results and experimental measurements of the effective thermal conductivity of the crushed fibers packed beds. The Schuetz and Glicksman analytical model [21], is applicable to porous media containing randomly oriented fibers. Considering the thermal conductivity of solid/fluid phase (k_{JM_s} , k_f) and the morphological parameter f_s of the solid phase (with $f_s = 1$ in the case of fiber particles), the effective thermal conductivity of the crushed fibers is determined using the following expression:

$$k_{JM,eff} = \phi_{inter}k_f + (1 - \phi_{inter}) \times \left(\frac{2 - f_s}{3}\right)k_{JM_s} \tag{13}$$

Where

- k_f is the thermal conductivity of the fluid phase (air)
- k_{JM_s} is the local thermal conductivity of Juncus maritimus fibers
- ϕ_{inter} is the porosity between the particles
- $k_{JM,eff}$ is the effective thermal conductivity of the packed bed of the crushed fibers

The local thermal conductivity of Juncus maritimus particles estimated from Glicksman model (Equation (13)) and crushed fibers packed beds effective thermal conductivity measurement is

$$k_{JM_s} = \frac{3}{2 - f_s} \frac{k_{JM,eff} - \phi_{inter}k_f}{1 - \phi_{inter}} = 0.719 \text{ W/m}\cdot\text{K} \tag{14}$$

A recent model, proposed by Nguyen et al. [22] is also used to identify the local thermal conductivity of Juncus maritimus fibers. This model is based on the Self-consistent scheme, it was previously applied to model the thermal conductivity of hemp insulation material.

$$k_{JM_s} = \frac{3k_{JM,eff}}{1 + \frac{\phi_{inter}}{1 - \phi_{inter}} \times \frac{k_f - k_{JM,eff}}{k_f + 2k_{JM,eff}}} - 2k_{JM,eff} \tag{15}$$

The local thermal conductivity of Juncus maritimus fibers estimated from Equation (15) and crushed fibers packed beds effective thermal conductivity measurement is $k_{JM_s} = 0.8 \text{ W/m}\cdot\text{K}$. The relative deviation between the estimated values using Equation (13) or (15) does not exceed 6%. It can be concluded that models are in good agreement. A mean value $k_{JM_s} = 0.76 \text{ W/m}\cdot\text{K}$ can be considered in the next.

It is important to note that radiation heat transfer inside the porous material could contribute to the total heat transfer measured due to the high porosity (70%). Thus, we can retain that the local thermal conductivity of Juncus maritimus fibers identified could be overestimated using this method. Radiation contribution is often neglected in previous works dealing with local solid thermal conductivity determination for hemp insulation materials and other bio based materials [8,22]. However, it can be noted that for traditional porous insulating media used in building application

(such as polystyrene foam at ambient temperature), radiation contribution can reach 35% of the total effective thermal conductivity.

3.4.3. Effective Thermal Conductivity of the Composite Samples/Experimental and Analytical Results

Analytical Models

3D- μ CT image of composite samples (Figure 5c,d) show, heterogeneous medium with fibers randomly distributed in the mortar matrix.

An estimate of the effective thermal conductivity of composite samples can obtain by the Geometric mean model [31]. This model uses the estimated thermal conductivities of each phase and their volume fractions. It can be noted that this model has been used to estimate the thermophysical properties of date palm fibers/gypsum composite [35].

The geometric mean model assumes random distribution of two components of the materials as a function of their volume fractions. Considering the mortar matrix as solid phase and the *Juncus maritimus* particles as dispersed phase, the effective thermal conductivity is calculated using the following expression:

$$k_{eff} = k_{JM_s}^{\varphi_{v, JM}} \times k_e^{(\phi + \varphi_{v, m})} \quad (16)$$

The Schuetz and Glicksman (Equation (17)) and Nguyen analytical models (Equation (18)) are applied to composites samples constituted of porous mortar and *Juncus maritimus* fibers.

$$k_{eff} = \frac{\varphi_{v, JM}}{3} k_{JM_s} + (\phi + \varphi_{v, m}) k_e \quad (17)$$

$$2k_{eff}^2 + k_{eff}(k_e(1 - 3(\phi + \varphi_{v, m})) - k_{JM_s}(2 - 3(\phi + \varphi_{v, m}))) - k_{JM_s}k_e = 0 \quad (18)$$

Experimental identification of local *Juncus maritimus* thermal conductivity from composite effective conductivity

Experimental results are compared with previous theoretical models using the identified local thermal conductivity, $k_{JM_s} = 0.76$ W/m·K, (obtained from crushed fibers effective thermal conductivity measurements and analytical model results) (Figure 7). It can be observed that there are non-negligible deviations between theoretical results. The Glickman, Geometric mean and Nguyen models overestimate experimental results of the effective thermal conductivity. These results tend to show that identified value of the local thermal conductivity, k_{JM_s} , is overestimated. These results could be explained by the non-negligible radiation heat transfer contribution in the crushed fibers sample which is taken into account in the k_{JM_s} value inducing overestimation.

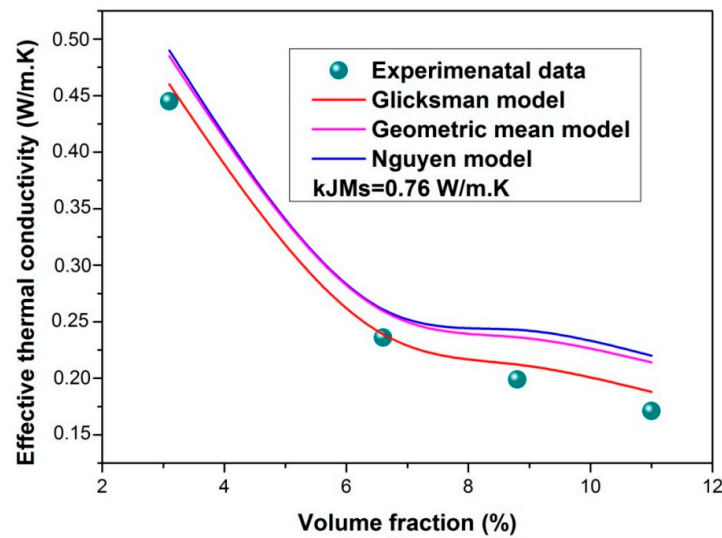


Figure 7. Experimental results compared with theoretical models calculated with $k_{JM_s} = 0.76 \text{ W/m}\cdot\text{K}$.

Alternatively, the JM local thermal conductivity of *Juncus maritimus* fibers was identified using analytical models and experimental measurements of thermal conductivity of composite samples for different *Juncus maritimus* volume fraction. The Glicksman, Geometric mean and Nguyen models are applied to composite samples constituted of mortar matrix and dispersed fibers. The estimated values of JM local thermal conductivity by these latter models are 0.472 ± 0.09 , 0.125 ± 0.028 and $0.130 \pm 0.033 \text{ W/m}\cdot\text{K}$, respectively. As expected the value are inferior to $k_{JM_s} = 0.76 \text{ W/m}\cdot\text{K}$ (obtained in Section 3.4.2). The relative deviations between the estimated values of local thermal conductivity of JM crushed fibers and of the JM fibers embedded in composite samples estimate by Equations (16)–(18) are 83.55%, 37.8%, and 83%, respectively. It seems that the *Juncus maritimus* local thermal conductivity estimated by Glicksman model is the most appropriate. The reduction is too large for the both other models and seems not realistic. Thus, the value k_{JM_s} is estimated to be $0.472 \text{ W/m}\cdot\text{K}$.

Using the thermal conductivity of porous mortar values, k_e , (Table 4) and the estimated local thermal conductivity of crushed *Juncus maritimus* fibers $k_{JM_s} = 0.472 \pm 0.09 \text{ W/m}\cdot\text{K}$, both Glicksman model and the effective thermal conductivity experimental data of composite samples are plotted in Figure 8. It is observed a good agreement between results for the different volume fraction.

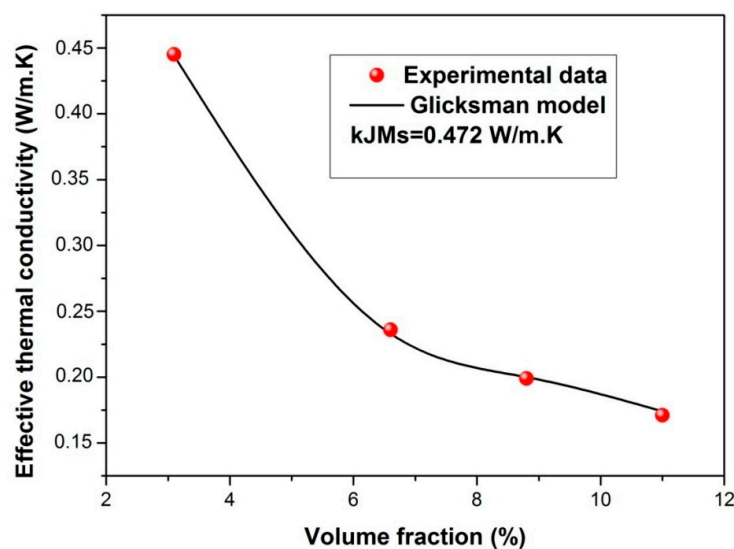


Figure 8. Comparison of JM/mortar composites effective thermal conductivity experimental results with Glicksman model calculated using the estimated $k_{JM_s} = 0.472 \text{ W/m}\cdot\text{K}$.

4. Conclusions

The thermal properties and microstructures characterizations of new insulating materials based on *Juncus maritimus* mortar composites were investigated. The thermal properties measurement was performed using boxes method and the microstructures characterization was studied using scanning electron microscope (SEM) and micro computed Tomography (μ CT) techniques. The results presented herein point out that the crushed *Juncus maritimus* fibers present low thermal conductivity, close to insulating materials such as wood shaving, date palm fibers (DPF). They could be used to replace the traditional reinforcement (such as glass fibers). A specific attention is put on the influence of *Juncus maritimus* fibers content.

It is shown that the increasing of the *Juncus maritimus* fibers content in the mortar induces increasing of porosity of mortar composite, porosity is almost two times higher than the reference mortar. Subsequently, the overall thermal conductivity is reduced by up to 67% for 10% of JM mass fraction in the mortar matrix; the thermal diffusivity is reduced by about 37% compared to reference mortar. Furthermore, the use of the *Juncus maritimus* particles as reinforcement in the mortar matrix decreases its density by up to 44%. As a result, these new lightened composites are shown to present efficient thermal performance materials. Thus the use of the natural material “*Juncus maritimus*” in the construction materials is promising. In future work the mechanical properties could be investigated and improved using chemical treatment of *Juncus maritimus* fibers.

We investigate also thermal conductivity analytical models of composites. The thermal conductivities of each solid phase constitutive of the materials are required. Such local conductivities are difficult to measure directly. The solid thermal conductivity of dense mortar is determined by fitting Hadley model results and experimental measurements of the effective thermal conductivity of the porous mortar samples without fibers. This method leads to the identification of the solid thermal conductivity of dense mortar, $k_s = 2.868 \text{ W/m}\cdot\text{K}$. Hence, the effective thermal conductivity of porous mortar is deduced theoretically by Hadley model for different porosities.

On the other hand, the local thermal conductivity of *Juncus maritimus* is particularly difficult to determine, such data are not available in literature. It is identified by fitting experimental effective conductivity of samples and analytical modeling results. Effective thermal conductivity measurements are performed on packed bed of crushed fibers but also on mortar composites samples. Both measurements are complementary and are recommended in order to analyze the results, to guide the identification of local thermal conductivity of *Juncus maritimus* and to choose the most appropriate analytical models.

Indeed, measurement of effective thermal conductivity performed on packed bed of crushed fibers permit to obtain a first estimation of k_{JMs} . We have shown that this value $k_{JMs} = 0.76 \text{ W/m}\cdot\text{K}$ could be overestimated due to the radiative contribution. Thus, we can deduce that the value of k_{JMs} identified from mortar composites samples must be lower than the first estimation of k_{JMs} . It was deduced that the Glicksman model is the most appropriate model and an estimated value of $0.472 \text{ W/m}\cdot\text{K}$ for local thermal conductivity of *Juncus maritimus* is obtained.

Author Contributions: Investigation and writing-original draft Z.S.; Methodology, Z.S.; D.B. and A.J.; Supervision and validation, D.B., A.J., N.N. and N.B.

Funding: This research received no external funding.

Conflicts of Interest: The authors declare no conflict of interest.

Nomenclature

R	electrical resistance (Ω)
q	heat flow (W/m^2)
C	heat loss coefficient $W \cdot ^\circ C^{-1}$
e	Thickness (m)
S	Surface (m^2)
T	Temperature ($^\circ C$)
k	Thermal conductivity ($W/m \cdot K$)
U	Voltage (V)
V	Volume (m^3)

Greek symbols

ρ	density (kg/m^3)
φ_m	mass fraction
ϕ	porosity
α	Thermal diffusivity (m^2/s)
φ_v	volume fraction

Subscripts

a,JM	Apparent crushed Juncus maritimus
c	composite
JM,eff	crushed JM fibers packed bed
0	dry
eff	effective
f	fluid phase
inter	interparticle
JM	Juncus maritimus fibers
JMs	local
mes	measured
P	pores
e	porous mortar
P	Plexiglas
s	solid phase
m	Sand and cement matrix
t	total

References

1. Ben Mansour, N.; Boudjemaa, A.; Gherabli, A.; Kareche, A.; Boudenne, A. Thermal and mechanical performance of natural mortar reinforced with date palm fibers for use as insulating materials in building. *Energy Build.* **2014**, *81*, 98–104. [[CrossRef](#)]
2. Chikhi, M.; Agoudjil, B.; Boudenne, A.; Gherabli, A. Experimental investigation of new biocomposite with low cost for thermal insulation. *Energy Build.* **2013**, *66*, 267–273. [[CrossRef](#)]
3. Baillis, D.; Coquard, R.; Moura, L.M. Heat transfer in cellulose-based aerogels: Analytical modelling and measurements. *Energy* **2015**, *84*, 732–744. [[CrossRef](#)]
4. Coquard, R.; Baillis, D. Thermal conductivity of Kelvin cell cellulosic aerogels: Analytical and Monte Carlo approaches. *J. Mater. Sci.* **2017**, *52*, 11135–11145. [[CrossRef](#)]
5. Collet, F.; Pretot, S. Thermal conductivity of hemp concretes: Variation with formulation, density and water content. *Constr. Build. Mater.* **2014**, *65*, 612–619. [[CrossRef](#)]
6. Evrard, A.; De Herde, A. Hydrothermal Performance of Lime–Hemp Wall Assemblies. *J. Build. Phys.* **2009**, *34*, 5–25. [[CrossRef](#)]
7. Tran Le, A.D.; Maalouf, C.; Mai, T.H.; Wurtz, E.; Collet, F. Transient hygrothermal behavior of a hemp concrete building envelope. *Energy Build.* **2010**, *42*, 1797–1806. [[CrossRef](#)]
8. Rahim, M.; Douzane, O.; Tran Le, A.D.; Langlet, T. Effect of the moisture and temperature on thermal properties of three bio-based materials. *Constr. Build. Mater.* **2016**, *111*, 119–127. [[CrossRef](#)]

9. Cherki, A.; Remy, B.; Khabbazi, A.; Jannot, Y.; Baillis, D. Experimental thermal properties characterization of insulating cork-gypsum composite. *Constr. Build. Mater.* **2014**, *54*, 202–209. [[CrossRef](#)]
10. Barreca, F.; Fichera, C.R. Thermal insulation performance assessment of agglomerated cork boards. *Wood Fiber Sci.* **2016**, *48*, 96–103.
11. Agoudjil, B.; Benchabane, A.; Boudenne, A.; Ibos, L.; Fois, M. Renewable materials to reduce building heat loss: Characterization of date palm wood. *Energy Build.* **2011**, *43*, 491–497. [[CrossRef](#)]
12. Boumhaout, M.; Boukhattem, L.; Hamdi, H.; Benhamou, B. Thermomechanical characterization of a bio-composite building material: Mortar reinforced with date palm fibers mesh. *Constr. Build. Mater.* **2017**, *13*, 241–250. [[CrossRef](#)]
13. Korjenic, A.; Petránek, V.; Zach, J.; Hroudová, J. Development and performance evaluation of natural thermal-insulation materials composed of renewable resources. *Energy Build.* **2011**, *43*, 2518–2523. [[CrossRef](#)]
14. Osseni, S.; Ahouannou, C.; Sanya, E.A.; Jannot, Y. Investigation on the use of the cement mortar containing banana fibers as thermal insulator building. *Int. J. Adv. Res.* **2016**, *4*, 1142–1152. [[CrossRef](#)]
15. Belkhrchouche, D.; Chaker, A. Effects of moisture on thermal conductivity of the lightened construction material. *Int. J. Hydrogen Energy* **2016**, *41*, 7119–7125. [[CrossRef](#)]
16. Hashin, Z. Assessment of the Self Consistent Scheme Approximation: Conductivity of Particulate Composites. *J. Compos Mater.* **1968**, *2*, 284–300. [[CrossRef](#)]
17. Krischer, D.; Kroll, K. *Technique de Séchage, Centre Technique des Industries Aérouliques et Thermiques*; Springer: Berlin, Germany, 1963; pp. 86–214.
18. Nguyen, T.T. Contribution à L'étude de la Formulation et du Procédé de Fabrication D'élément de Construction en Béton de Chanvre. Ph.D. Thesis, Bretagne Sud University, Bretagne Sud, France, 2010.
19. Cerozo, V. Propriétés Mécanique, Thermique et Acoustique d'un Matériau à Base de Particules Végétales, Approche Expérimentale et Modélisation Théorique. Ph.D. Thesis, Lyon University, Lyon, France, 2005.
20. Lisse, P.; Louis, A. *A Nabeul, Les Nattiers et Les Nattes, Etude Technique et Sociale D'artisanat Tunisien*; Institut des Belles Lettres Arabes: Tunis, Tunisia, 1954; pp. 1–45.
21. Schuetz, M.A.; Glicksman, L.R. A basic study of heat transfers through foam insulation. *J. Cell Plast.* **1984**, *20*, 114–121. [[CrossRef](#)]
22. Nguyen, S.T.; Tran-Le, A.D.; Vu, M.N.; To, Q.D.; Douzane, O.; Langlet, T. Modeling thermal conductivity of hemp insulation material: A multi-scale homogenization approach. *Build. Environ.* **2016**, *107*, 127–134. [[CrossRef](#)]
23. Woodside, W.; Messmer, J.H. Thermal conductivity of porous media I. Unconsolidated sands. *J. Appl. Phys.* **1961**, *32*, 1688–1698. [[CrossRef](#)]
24. Hamza, S.; Saad, H.; Charrier, B.; Ayed, N.; Charrier-El Bouhtoury, F. Physico-chemical characterization of Tunisian plant fibers and its utilization as reinforcement for plaster based composites. *Ind. Crop. Prod.* **2013**, *49*, 357–365. [[CrossRef](#)]
25. NT 47-01:1983—*Tunisian Standard Specification of Ordinary Portland*; Journal Officiel de la République Tunisienne N°70; Imprimerie Officielle De La République Tunisienne: Mégrine, Tunisia, 1983; p. 3178.
26. EN 197-1:2000—*European Standard Specification of Ordinary Portland*; European Committee Standardization: Brussels, Belgium, 2000.
27. Anovitz, L.M.; Cole, D.R. Characterization and analysis of porosity and pore structures. *Rev. Mineral.Geochem.* **2015**, *80*, 61–64. [[CrossRef](#)]
28. Taoukil, D.; Elbouardi, A.; Sick, F.; Mimet, A.; Ezbakhe, H.; Ajzoul, T. Moisture content influence on the thermal conductivity and diffusivity of wood-concrete. *Constr. Build. Mater.* **2013**, *48*, 104–115. [[CrossRef](#)]
29. Martin, B. Etude de L'anisotropie de la Conductivité des Super-Isolants. Ph.D. Thesis, University of Lorraine, Lorraine, France, 1988.
30. Yezou, R. Contribution à L'étude des Propriétés Thermophysiques des Matériaux de Construction Cohérents et non cohérents. Ph.D. Thesis, University of Lyon, Lyon, France, 1978.
31. Taoukil, D.; El-bouardi, A.; Ezbakhe, H.; Ajzoul, T. Thermal Properties of Concrete Lightened by Wood Aggregates. *Res. J. Appl. Sci. Eng. Technol.* **2011**, *3*, 113–116.
32. Panesar, D.K.; Shindman, B. The mechanical, transport and thermal properties of mortar and concrete containing waste cork. *Cem. Concr. Compos.* **2012**, *34*, 982–992. [[CrossRef](#)]

33. Baouche, N.; Baynast, H.; Lebert, A.; Sun, S.; Mingo, C.; Leclaire, P.; Michaud, P. Mechanical, thermal and acoustical characterizations of an insulating bio-based composite made from sunflower stalks particles and chitosan. *Ind. Crop. Prod.* **2014**, *58*, 244–250. [[CrossRef](#)]
34. Kaviany, M. *Principles of Heat Transfer in Porous Media*; Springer: New York, NY, USA, 1991; pp. 1–626.
35. Braiek, A.; Karkri, M.; Adili, A.; Ibos, L.; Nasrallah, S. Estimation of the thermophysical properties of date palm fibers/gypsum composite for use as insulating materials in building. *Energy Build.* **2017**, *140*, 268–279. [[CrossRef](#)]



© 2019 by the authors. Licensee MDPI, Basel, Switzerland. This article is an open access article distributed under the terms and conditions of the Creative Commons Attribution (CC BY) license (<http://creativecommons.org/licenses/by/4.0/>).